E. SMIRNOV[1,3]
M. STEPIĆ[1,2]
V. SHANDAROV[3]
D. KIP[1,✉]

Pattern formation by spatially incoherent light in a nonlinear ring cavity

[1] Institute of Physics and Physical Technologies, Clausthal University of Technology,
  38678 Clausthal-Zellerfeld, Germany
[2] Vinča Institute of Nuclear Sciences, P.O.B. 522, 11001 Belgrade, Serbia and Montenegro
[3] State University of Control Systems and Radioelectronics, 40 Lenin Ave., 634050 Tomsk, Russia

ABSTRACT Modulation instability and pattern formation by spatially incoherent light is investigated experimentally in a nonlinear ring cavity using a photorefractive strontium barium niobate crystal as the nonlinear medium. A step-like threshold for the onset of pattern formation is observed experimentally for the case of high optical feedback. When compared to the case without feedback, this threshold is shifted towards smaller nonlinearities and a significant increase of the modulation degree of the obtained patterns is obtained. Our measurements also show that, above threshold, the dominating spatial frequency of the patterns decreases monotonically with both increasing nonlinearity and increasing feedback.

PACS 42.65.Tg; 42.65.Sf; 89.75.Kd

1   Introduction

The formation of regularly ordered patterns is a universal feature of many nonlinear systems. Among a large number of different systems in physics [1, 2], chemistry [3, 4], and biology [5, 6], formation of patterns has been intensively studied in optics, including lasers and nonlinear optical devices [2, 7–9]. The reason is that optical systems, which are relatively simple both in experimental realization and in their mathematical description, provide excellent opportunities for the investigation of their general nonlinear dynamics. On one hand, the phenomenon of spontaneous pattern formation is closely related to the appearance of modulation instability (MI) [10, 11]: in an extended nonlinear medium, an initially uniform intensity distribution becomes unstable during propagation through the medium, i.e. it breaks up into filaments of light, where each single filament or spot can be regarded as a spatial soliton. On the other hand, both isolated and periodic patterns may form as a consequence of optical feedback using reflecting mirrors or cavities. These processes can be observed in a large variety of nonlinear optical systems, including both purely conservative systems [12] and those that exhibit a certain degree of dissipation [2, 13]. In the latter case, formation of transverse patterns and spatial

solitons (so-called cavity solitons) in the dissipative environment of nonlinear cavities (e.g. gas-filled optical resonators and semiconductors) has attracted much attention in the past years [14].

Both spontaneous and feedback-driven optical pattern formation (as well as MI) have been mostly investigated using spatially and temporally coherent light. However, some years ago it was demonstrated that MI and spontaneous pattern formation can also occur in a large variety of weakly correlated nonlinear systems, in particular in non-instantaneous nonlinear optical systems using spatially incoherent light [15, 16]. A specific feature is the existence of a well-defined threshold for the appearance of MI in such systems (whereas no such threshold exists for MI using coherent light) that is set by the coherence properties of the light. Intuitively, this threshold can be understood as the balance point of two competing processes: the growth of periodic perturbations on top of a uniform wavefront and the diffusive linear washout of this modulation due to the limited coherence of the light. It has been shown both theoretically and experimentally that the spatial frequencies of the regular optical patterns are directly related to the coherence properties of the light and the magnitude of the nonlinearity.

Recently, it was demonstrated that patterns may also occur in a passive nonlinear cavity using spatially incoherent light [17, 18]. Different to systems with fully coherent feedback (like most single-mirror systems) where interference of forward and backward propagating beams leads to reflection gratings in the nonlinear medium, the arising spatial frequencies of the patterns are now determined by both the (single-pass) MI process as well as the quality factor and spatial bandwidth of the incoherent cavity. Therefore, regarding the visibility of the obtained patterns in a nonlinear incoherent cavity, two different thresholds may be distinguished. The first (MI) threshold is determined by the MI process itself (leading to one-dimensional (1D) stripe patterns) and exists also for the case without feedback, i.e. it does not depend on the cavity properties. As this process starts from noise containing many competing spatial frequencies, the observed threshold is relatively smooth. The second (cavity) threshold is determined by the interplay of nonlinear gain and cavity loss. Depending on the quality factor of the cavity, it may lead to a sharp increase of the pattern's visibility for higher feedback, similar to many coherent feedback systems. Obviously, for a fixed value

✉ Fax: +49 5323 72 2175, E-mail: d.kip@pe.tu-clausthal.de

of the spatial coherence length, the cavity threshold is always lower than the MI threshold. We also note that at an additional (higher) threshold one may observe the formation of regular two-dimensional (2D) structures [16, 19, 20], which is a direct consequence of the anisotropy of the nonlinear material (e.g. in photorefractive crystals).

However, in recent experiments conducted with partially spatially coherent light only a smooth and relatively small increase of the visibility of patterns as a function of feedback has been measured [18] that did not allow for a distinction of MI and cavity thresholds, this probably being a consequence of a too low feedback of the cavity. Furthermore, no results on the observed spatial frequencies of the patterns above threshold have been reported. In this contribution we investigate a ring cavity with significantly higher feedback. We observe slightly different thresholds for the cases with and without feedback, and a decrease of the dominating spatial frequency above threshold. In Sect. 2 we describe our setup and comment on physically important variables and parameters of the system. Section 3 is devoted to experimental results and their discussion.

2   Experimental setup

Our experimental setup that is sketched in Fig. 1 is a passive ring cavity with a biased photorefractive SBN61 ($Sr_{0.61}Ba_{0.39}Nb_2O_6$) crystal doped with 200 ppm Rh as the nonlinear element.

The length of the SBN61 crystal is 4.8 mm along the light propagation direction, while the ferroelectric c-axis is directed perpendicular to the propagation direction. It is important to note that this sample has as-grown surfaces with nearly perfect flatness and is optically homogeneous with almost no visible striations. An electric field $E_0 = U/d$ (where U is the applied voltage and $d = 4.8$ mm) can be applied along the c-axis using silver-paste electrodes. In this way, one can tune the strength of the screening photorefractive nonlinearity, which is proportional to $\Delta n = -0.5 r_{33} n_e^3 E_{sc}$, by changing the applied electric field [16]. This nonlinearity is of saturable type due to the limited number of charge traps inside the crystal, i.e. a limited value of the internal electric drift field E_{sc}.

In the experiments we use an argon-ion laser whose green line ($\lambda = 514.5$ nm) is extraordinarily polarized in order to utilize the largest nonlinear electro-optic coefficient r_{33} of the SBN61 crystal. This polarized signal light beam passes

a rotating diffuser, thus making it partially spatially incoherent, and is finally collimated by virtue of lens L2 in order to uniformly illuminate the whole sample. The sample is additionally illuminated from the top using light of an incendescent light bulb. This background beam serves merely to set the degree of saturation of the photorefractive screening nonlinearity. An advantage of this setup, in comparison to the corresponding one in [18], is that the background beam, which has an intensity I_b, does not have to be recycled in the cavity. We use high-reflecting dielectric mirrors and beam splitters that are optimized for the polarization of the signal beam to build the cavity, and thus obtain a maximized optical feedback. A sensitive current meter measures the photocurrent through the crystal, thus monitoring the photoconductivity that is generated by the signal beam, the background beam, or both beams together. In this way, an intensity ratio of one is obtained by adjusting the corresponding light intensities in order to generate the same photoconductivity of the sample.

The ring cavity consists of two dielectric beam splitters (reflectivity $R = 0.7$ for in-coupling and $R = 0.98$ for out-coupling of light, respectively), two dielectric mirrors with $R = 0.995$, and four anti-reflection-coated lenses with focal lengths $f = 10$ cm forming two $4f$ systems, giving the length of the cavity feedback loop of 80 cm. Taking Fresnel reflections of the SBN sample into account, an optical feedback ε of about 45% is obtained. The other inherent lengths of this $4f$ low-finesse imaging system are the temporal coherence length of the light used (≈ 5 cm) and the length of the photorefractive crystal in the cavity. A small part of the light inside the cavity is transmitted through the second beam splitter, and an additional lens is used to image the crystal's end face onto a CCD camera. To adjust the ring cavity, we image a thin wire (placed at the center of the nonlinear medium) that serves as a control object back on itself [18]. When imaged onto the CCD camera, the control image becomes brighter due to the feedback in the system. By carefully adjusting the overlap of consecutive control images from different cycles of the cavity, beam translations and tilts can be avoided.

3   Experimental results

In all measurements we have adjusted the intensity ratio of signal and background light intensities to be $I/I_b \approx 1$. For measurements with cavity the optical feedback was held at a constant level of $\varepsilon \approx 45\%$, which was the maximum possible value that is mainly restricted by the reflectivity of the beam splitter used for the input signal light. The spatial coherence length can be adjusted by changing the spot size of the laser beam on the rotating diffuser with the help of lens L1. By measuring the mean speckle size (when the diffuser is stopped) on the crystal input facet, the spatial coherence length is adjusted to be $l_c \approx 10$ µm in all experiments.

In Fig. 2 measured intensity patterns at the output facet of the sample for different values of the externally applied voltage are shown. In the top row images obtained without feedback are given, while in the bottom row the corresponding images with feedback are presented. Above 1D MI and cavity thresholds, respectively, regularly spaced stripes that are inclined by $\approx 45°$ are observed. It is important to note that an initial orientation of stripes perpendicular to the c-axis, as was
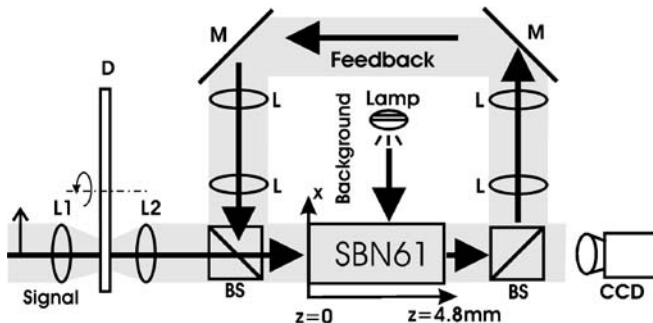
FIGURE 1 Experimental setup: D, rotating diffuser; L, L1, L2, lenses; BS, beam splitters; M, dielectric mirrors; CCD, CCD camera
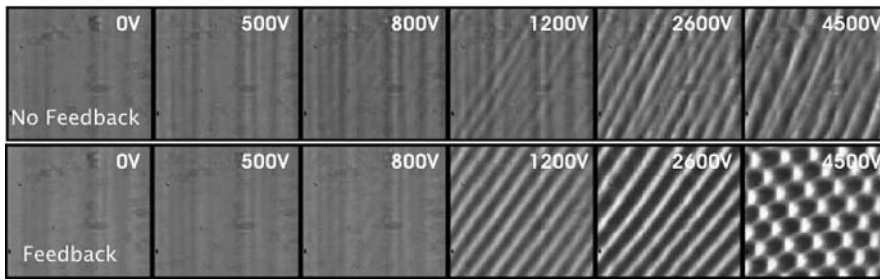
FIGURE 2 Experimentally obtained intensity patterns at the rear facet of the nonlinear crystal. *Top row*: without feedback; *bottom row*: constant feedback $\varepsilon \approx 45\%$

observed in former works [16, 18] where this behavior was related to striations of the sample, is almost absent here.

The experimentally obtained dependence of the visibility of the pattern, described by the modulation $m = (I_{max} - I_{min})/(I_{max} + I_{min})$, on the applied voltage both with and without feedback is given in Fig. 3. According to [17], our system is in the state ($\varepsilon \approx 45\%$, $l_c \approx 10\,\mu m$, $I/I_b \approx 1$), where the first threshold (1D MI) and the second (cavity threshold) should be distinguishable. Indeed, in the case without feedback the first signs of weak 1D MI can be observed for an applied voltage of $U = 750\,V$, which is at least partially related to amplification of pre-dominant spatial frequencies that are due to very weak striations in the sample. However, a faster increase of the modulation is observed later in the voltage range 1500–2000 V. Above this range, the modulation increases only slowly and reaches maximum values of about 40%. On the other hand, for the case with feedback the cavity threshold, which appears when the nonlinear gain overcomes the loss in a single cavity pass, is observed for an applied voltage of $U = 900\,V$, where the modulation sharply increases from almost zero to values of about 70%. This is in good agreement with the theoretical model in [17] (Fig. 2), where for strong feedback an abrupt increase of the modulation depth is predicted. A specific feature of the cavity system containing a saturable nonlinear medium is the fact that, for a higher degree of saturation, feedback can suppress modulation instability. In our case the intensity ratio was fixed to a relatively high value of about one, and MI may be partly suppressed in the voltage range of 750–900 V, which is in accordance with the theoretical model [17].
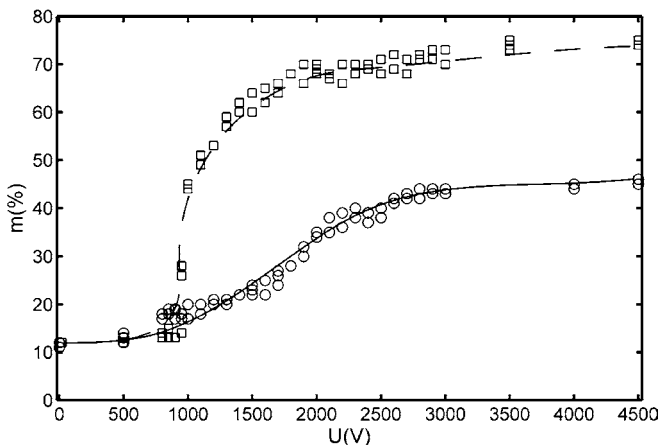
Regularly spaced 2D structures in the ring cavity start to appear at $U \approx 3000\,V$ and finally cover the whole sample at a voltage of $U \approx 4500\,V$, which is close to the short-circuit current limit of our sample (surrounded by air, $E_{max} \approx 10\,kV/cm$). Here, it is interesting to note that, for high applied electric fields E_0, i.e. large nonlinearity, the 2D MI patterns not only show chess-like or square patterns, but may also contain hexagonal sub-structures. An example of such a pattern is shown in Fig. 4. On the other hand, for the parameters used here no 2D structures are observed for the case without feedback, i.e. for single-pass MI.

The dominating spatial frequency ν of the emerging patterns is determined by virtue of multiple line scans of the images measured by the CCD camera. For each value of the applied voltage we conducted four independent measurements and plot the averaged value of the spatial frequency as a function of voltage in Fig. 5. Because of the quite low visibility in the region of the MI and cavity thresholds, the corresponding data are not included in this figure. However, in this region the dominating spatial frequency increases with applied voltage to some finite value. In Fig. 5 one can immediately notice that the dominating spatial frequency, both with and without feedback, is a decreasing function of nonlinearity. Furthermore, the feedback significantly decreases the dominating spatial frequency of the emerging patterns when compared to the case without feedback. The fact that these frequencies are non-monotonic functions of the applied voltage

FIGURE 3   Visibility (modulation depth m) of emerging patterns for different values of applied voltage U (nonlinearity) without feedback (*circles*) and with feedback $\varepsilon \approx 45\%$ (*squares*). The *lines* are only guides to the eye
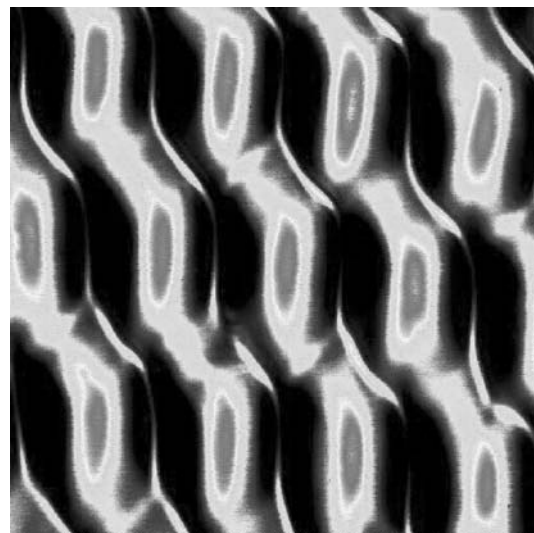
FIGURE 4   Hexagonal sub-structures observed for incoherent MI in a nonlinear biased SBN sample above the 2D threshold
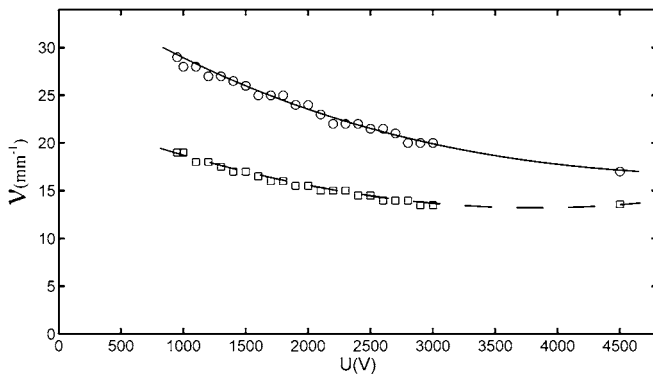
FIGURE 5 Dominating spatial frequency ν of the emerging pattern as a function of applied voltage U for the cases without feedback (*circles*) and with feedback (*squares*). The *lines* are only guides to the eye

(or nonlinearity) has been reported in [16] (Fig. 5), where it was shown that the dominating spatial frequency increases in the region of small refractive-index changes, reaches a maximum, and then decreases. It has been discussed in [16] that this phenomenon may be related to an ordering in the system while approaching the 2D MI threshold. Here we show that this decrease of the spatial frequency also occurs in a parameter range (without feedback) where the 2D MI threshold is still absent. Obviously, these experimental findings are not supported by the 1D theoretical modeling in [15], where an increase is predicted with both growing nonlinearity and growing saturation ratio of signal and background intensities.

4   Conclusion

To summarize, we studied incoherent light propagation in a nonlinear ring cavity with high feedback, and compared the results with the single-pass case without feedback. We observed a sharp threshold for the case with feedback, which may be related to the almost striation-free SBN sample that causes only little initial noise. When the feedback is blocked, only a smooth increase of visibility of 1D patterns is found with a smaller modulation degree for high nonlinearity. Furthermore, above threshold we observed a strong decrease of the pattern's spatial frequency both for single-pass and cavity experiments, which seems to be related rather to a change of spatial coherence of the propagating light than to the influence of crystal striations.

REFERENCES

1 L. Spinelli, G. Tissoni, M. Brambilla, F. Prati, L.A. Lugiato, Phys. Rev. A **58**, 2542 (1998)
2 F.T. Arecchi, S. Boccaletti, P.L. Ramazza, Phys. Rep. **318**, 1 (1999)
3 A.N. Zaikin, A.M. Zhabotinsky, Nature **225**, 535 (1970)
4 K.J. Lee, W.D. McCormick, J.E. Pearson, H.L. Swinney, Nature **369**, 215 (1994)
5 A.M. Turing, Philos. Trans. R. Soc. London B **237**, 37 (1952)
6 P.K. Maini, K.J. Painter, H.N.P. Chau, J. Chem. Soc. **93**, 3601 (1997)
7 N.B. Abraham, W.J. Firth, J. Opt. Soc. Am. B **7**, 951 (1990)
8 T. Ackemann, W. Lange, Appl. Phys. B **72**, 21 (2001)
9 S.J. Jensen, M. Schwab, C. Denz, Phys. Rev. Lett. **81**, 1614 (1998)
10 V.I. Bespalov, V.I. Talanov, JETP Lett. **3**, 307 (1966)
11 L. Bergé, Phys. Rep. **303**, 260 (1998)
12 B.A. Malomed, D. Mihalache, F. Wise, L. Torner, J. Opt. B **7**, R53 (2005)
13 P. Grelu, J.M. Soto-Crespo, N. Akhmediev, Opt. Express **13**, 9352 (2005)
14 C.O. Weiss, M. Vaupel, K. Staliunas, G. Slekys, V.B. Taranenko, Appl. Phys. B **68**, 151 (1999)
15 M. Soljačić, M. Segev, T. Coskun, D.N. Christodoulides, A. Vishwanath, Phys. Rev. Lett. **84**, 467 (2000)
16 D. Kip, M. Soljačić, M. Segev, E. Eugenieva, D.N. Christodoulides, Science **290**, 495 (2000)
17 H. Buljan, M. Soljačić, T. Carmon, M. Segev, Phys. Rev. E **68**, 016616 (2003)
18 T. Carmon, H. Buljan, M. Segev, Opt. Express **12**, 3481 (2004)
19 D. Kip, M. Soljačić, M. Segev, S.M. Sears, D.N. Christodoulides, J. Opt. Soc. Am. B **19**, 502 (2002)
20 B. Gütlich, T. König, C. Denz, K. Motzek, F. Kaiser, Opt. Commun. **255**, 57 (2005)